Proceedings of the 7th European VLBI Network Symposium
Bachiller, R. Colomer, F., Desmurs, J.F., de Vicente, P. (eds.)
October 12th-15th 2004, Toledo, Spain

The asymmetric compact jet of GRS 1915+105

M. Ribó[1], V. Dhawan[2], and I. F. Mirabel[1,3]

[1] Service d'Astrophysique, CEA Saclay, Bât. 709, L'Orme des Merisiers, 91191 Gif-sur-Yvette, Cedex, France
[2] National Radio Astronomy Observatory, Socorro, NM 87801, USA
[3] Instituto de Astronomía y Física del Espacio, CONICET, C.C.67, Suc. 28, 1428 Buenos Aires, Argentina

Abstract. We present multiepoch VLBA observations of the compact jet of GRS 1915+105 conducted at 15.0 and 8.4 GHz during a *plateau* state of the source in 2003 March-April. These observations show that the compact jet is clearly asymmetric. Assuming an intrinsically symmetric continuous jet flow, using Doppler boosting arguments and an angle to the line of sight of $\theta = 70°$, we obtain values for the velocity of the flow in the range 0.3–0.5c. These values are much higher than in previous observations of such compact jet, although much lower than the highly relativistic values found during individual ejection events. These preliminary results are compatible with current ideas on the jet flow velocity for black holes in the low/hard state.

1. Introduction

GRS 1915+105 is a well-known microquasar containing a very massive stellar-mass black hole of $M = 14 \pm 4\ M_\odot$ (Greiner et al. 2001). During major flares it shows discrete relativistic ejection events with a velocity in the range 0.90–0.98c, inferred from VLA and MERLIN observations and assuming a distance to the source of $\simeq$12 kpc (see Mirabel & Rodríguez 1994 and Fender et al. 1999, respectively). On the other hand, when the source is in the so-called *plateau* state, a compact radio jet with a much lower velocity of 0.1c has been found in previous VLBA observations (Dhawan et al. 2000). We observed the source with the VLBA of the NRAO[1] during three epochs on spring 2003, as part of a multiwavelength campaign presented in Fuchs et al. (2003). Here we present a preliminary analysis of the obtained VLBA images.

2. Observations and results

We observed GRS 1915+105 with the VLBA at 15.0 and 8.4 GHz on 2003 March 24, April 2 and April 19 (runs A, B and C, respectively). A summary of the time intervals of our observations is presented in Table 1. The source 1923+210 was used as fringe-finder, while J1924+154 was used for phase-referencing the observations of GRS 1915+105 and the check source J1922+084. Cycle times of 3 minutes were used at both frequencies. The observations were conducted at 256 Mb s^{-1}, with 8 baseband channels and 2 bit sampling using both polarizations (modes `v2cm-256-8-2.set` and `v4cm-256-8-2.set`). This provided tape passes of 22 minutes at each frequency, that included a scan on the fringe-finder, 5 cycles on the target source and 1 cycle on the check source. We alternated 15.0 and 8.4 GHz passes, and we could include a total of 8, 6 and 11 passes on runs A, B and C, respectively. The data were processed at the VLBA correlator in Socorro, with an integration time of 2 s.

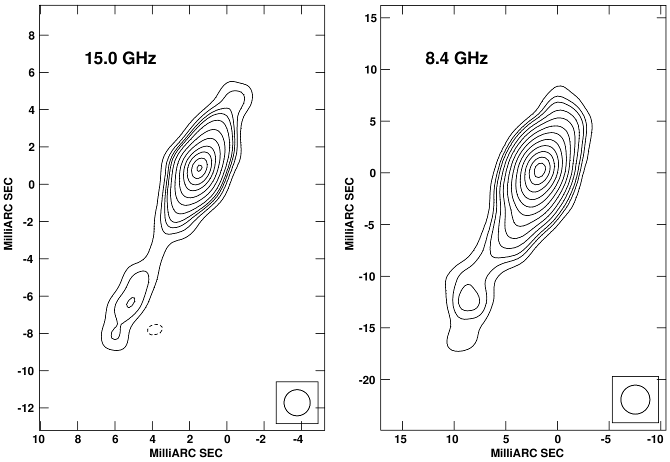

Fig. 1. VLBA images at 15.0 and 8.4 GHz obtained on 2003 April 19. The rms noise of the images are 0.19 and 0.08 mJy beam^{-1}, respectively, and contour levels start with −5, 5, 10, 15 times the rms noise. Notice the different scale used in each image.

The data reduction was performed using standard procedures within the AIPS software package of NRAO. We used the following parameters to produce the images: a weighting value for robust of −1, a cellsize of 0.15 and 0.30 mas, and a uv-tapering of 120 and 60 kλ at 15.0 and 8.4 GHz, respectively. Several phase self-calibration steps using boxes along the jet direction were performed, as well as careful editing of bad data after the first iterations. We produced final images by using a circular beam with a Full Width at Half Maximum (FWHM) equal to the average of the geometric means of the FWHM of the beams at all epochs: 1.4 and 2.8 mas at 15.0 and 8.4 GHz, respectively. All the obtained images reveal a jet-like feature, with a slightly asymmetric compact component brighter to the southeast (the approaching part of the jet) plus a further elongation towards the southeast. As an example, we show in Fig. 1 the images obtained at both frequencies during run C.

We also conducted VLA observations of GRS 1915+105 at 22 and 8.4 GHz during the first hour of run A, at 8.4 GHz during the first hour of run B, and again at 22 and 8.4 GHz just

[1] The National Radio Astronomy Observatory is a facility of the National Science Foundation operated under cooperative agreement by Associated Universities, Inc.

Table 1. Summary of the VLBA observations. See text for a detailed explanation.

Run	MJD	UT		ν (GHz)	S_ν (mJy)	α	$S_{\nu\ \mathrm{app}}$ (mJy)	$S_{\nu\ \mathrm{rec}}$ (mJy)	$\beta\cos\theta$ (for $k=2$)	β (for $k=2$)	$\beta\cos\theta$ (for $k=3$)	β (for $k=3$)
A	52722.7	2003 Mar 24	15:30–18:30	15.0	131.4	+0.3±0.2	80.1	55.1	0.11±0.02	0.32±0.04	0.07±0.01	0.20±0.02
				8.4	108.3		63.2	46.0	0.09±0.01	0.27±0.03	0.06±0.01	0.17±0.01
B	52731.6	2003 Apr 02	13:00–15:00	15.0	122.7	+0.1±0.2	83.9	41.4	0.18±0.02	0.54±0.06	0.12±0.01	0.35±0.03
				8.4	115.8		63.5	53.3	0.05±0.01	0.13±0.02	0.03±0.01	0.09±0.01
C	52748.4	2003 Apr 19	08:30–12:40	15.0	112.0	+0.4±0.2	69.6	43.8	0.14±0.02	0.42±0.05	0.09±0.01	0.26±0.02
				8.4	88.4		55.2	33.5	0.15±0.02	0.45±0.06	0.10±0.01	0.28±0.02

one day before run C. The obtained lightcurves show a nearly constant flux density during each individual observation, consistent with the steady behavior found in both Ryle Telescope radio observations and *RXTE*/ASM X-ray count rate (see Fig. 2 in Fuchs et al. 2003). Therefore, the requirement of constant flux density for synthesis imaging is satisfied, but see a detailed discussion on the eventual problems related to a changing morphology during the observations in Dhawan et al. (2000).

To better study the asymmetry of the jet we proceeded in the following way. First we selected the Clean Components (CC) representing the jet on the final images, and exported them out of AIPS. Then we shifted their coordinates to have the maximum centered at (0,0). We finally rotated them by using the Position Angle (PA) of the jet, 155°, so the X coordinate of the CC is parallel to the jet direction defined positive towards the approaching jet, and the Y coordinate is perpendicular to it. We then added together the flux of all CC in the approaching jet, and we did the same for the receding one.

Assuming that the jet is intrinsically symmetric, and neglecting possible free-free absorption effects, we can obtain the product $\beta\cos\theta$, being β the velocity of the flow in units of the speed of light and θ the angle between the jet and the line of sight, by means of the equation:

$$\beta\cos\theta = \frac{\left(S_{\nu\ \mathrm{app}}/S_{\nu\ \mathrm{rec}}\right)^{1/(k-\alpha)} - 1}{\left(S_{\nu\ \mathrm{app}}/S_{\nu\ \mathrm{rec}}\right)^{1/(k-\alpha)} + 1}\,, \tag{1}$$

where $S_{\nu\ \mathrm{app}}$ and $S_{\nu\ \mathrm{rec}}$ are the flux densities of the approaching and receding jets, respectively, k equals 2 for a continuous jet and 3 for discrete condensations, and α is the spectral index defined as $S_\nu \propto \nu^{+\alpha}$. Since the equation above is only valid for fluxes measured at equal distances from the core, we have added to the flux density obtained with the CC for the receding jet, the quantity $n\times3\sigma$, being σ the rms noise in the image and n the result of dividing the difference in total distance of the approaching and receding jets by the FWHM of the beam.

We quote in Table 1 the obtained results, where S_ν is the total flux density of the jet, α has been computed from the S_ν values at both frequencies on a given epoch (we assume a standard error of 0.2), and $S_{\nu\ \mathrm{app}}$ and $S_{\nu\ \mathrm{rec}}$ correspond to the fluxes of the approaching and receding jets computed as explained above. We finally quote the derived values for $\beta\cos\theta$ for the continuous jet ($k = 2$) and for the less realistic case of discrete condensations ($k = 3$), together with the value of β derived by assuming an angle $\theta = 70°$ in each case (see Fender et al. 1999). Values within the quoted errors have been obtained by changing the PA of the jet by ±5°. Since the images reveal a continuous jet, we will only consider the $k = 2$ case. The obtained values of β are $\simeq 0.3$ for run A and $\simeq 0.4$ for run C, while very different values are obtained at different frequencies for run B, being around 0.5 at 15.0 GHz and around the much lower value of 0.1 at 8.4 GHz. This last result can be understood when inspecting the corresponding image because the maximum CC happens to be slightly towards the receding part of the jet, and only a small shift of 0.3 mas in the jet center would provide a value of $\beta = 0.38 \pm 0.04$.

3. Discussion and conclusions

In general we can say that with the procedure described above we obtain a value for the jet flow velocity of $\sim 0.4\,c$ when assuming $k = 2$ and $\theta = 70°$. Lower values of β are obtained for smaller angles θ, which should be used if the source is closer than 12 kpc (Fender et al. 1999; Chapuis & Corbel 2004). In any case, the obtained values are higher than the ones reported in Dhawan et al. (2000) for a similar compact jet, but still much lower than the highly relativistic values inferred in discrete ejection events. These preliminary results are compatible with the Lorentz factors of $\Gamma \lesssim 2$ allowed for compact radio jets if the empirical correlation found between X-ray/radio flux for black holes in the low/hard sate holds (Gallo et al. 2003). A detailed analysis of these observations and their implications will be presented in a forthcoming paper.

Acknowledgements. M.R. acknowledges support by a Marie Curie Fellowship of the European Community programme Improving Human Potential under contract number HPMF-CT-2002-02053, partial support by DGI of the Ministerio de Ciencia y Tecnología (Spain) under grant AYA2001-3092, as well as partial support by the European Regional Development Fund (ERDF/FEDER).

References

Chapuis, C., & Corbel, S. 2004, A&A, 414, 659
Dhawan, V., Mirabel, I. F., & Rodríguez, L. F. 2000, ApJ, 543, 373
Fender, R. P., Garrington, S. T., McKay, D. J., et al. 1999, MNRAS, 304, 865
Fuchs, Y., Rodriguez, J., Mirabel, I. F., et al. 2003, A&A, 409, L35
Gallo, E., Fender, R. P., & Pooley, G. G. 2003, MNRAS, 344, 60
Greiner, J., Cuby, J. G., & McCaughrean, M. J. 2001, Nature, 414, 522
Mirabel, I. F., & Rodríguez, L. F. 1994, Nature, 371, 46